

## THE GRAVITY FIELD IN FORCE STANDARD MACHINES

*M. Schilling<sup>1</sup>, L. Timmen<sup>1</sup>, and R. Kümme<sup>2</sup>*

<sup>1</sup>Leibniz Universität Hannover, Institut für Erdmessung, Hannover, Germany, [schilling@ife.uni-hannover.de](mailto:schilling@ife.uni-hannover.de)

<sup>2</sup>Physikalisch-Technische Bundesanstalt (PTB), Braunschweig, Germany

**Abstract:** The gravity acceleration  $g$  plays an important role in several physical quantities as provided by National Metrology Institutes. The unit of force is realized in dependence on  $g$  in force standard machines (FSM). We present the results of the combination of forward modeling and gravimetric observations to determine the absolute value of  $g$  inside the new 200 kN FSM of the Physikalisch-Technische Bundesanstalt (PTB). A model of the machine itself and gravimetric measurements, performed prior and after the installation of the FSM, are compared. The agreement is within  $10 \text{ nm/s}^2$ . The final uncertainty concerning  $g$  is  $1.2 \times 10^{-7}$  due to temporal variations typically neglected in force measurements.

**Keywords:** gravity, force standard machine, gravimetry, forward gravity modelling

### 1. INTRODUCTION

Knowledge of the absolute value of gravity  $g$ , its variation and derived quantities are of interest in metrology. The physical quantity force is realized by different principles. In deadweight force standard machines (FSM), the force is generated by the weights of masses of up to some hundred tonnes. Gravity  $g$  acts on these masses, generating forces in the N to MN range. The force  $F$  is calculated by the sum of the products of the masses  $m_i$  and gravity values  $g_i$  valid at the center of mass of the individual deadweight  $i$

$$F = \sum_{i=1}^n m_i g_i \left(1 - \frac{\rho_a}{\rho_{mi}}\right) \quad (1)$$

The latter expression in (1) considers the buoyancy. In the following we will focus on the determination of  $g_i$ . To calculate the force  $F$ , the  $g$ -value has to be determined inside the FSM at a position not accessible with gravimeters. Prior to the installation of such a FSM, absolute and relative gravimetry can measure  $g$  and its vertical gradients. However, the FSM itself changes the local gravity field due to its mass, which has to be considered in the gravimetric results. The Newtonian attraction of the FSM masses and their effect on the vertical gradient can be calculated on the basis of, e.g., a 3D CAD model of the machine.

### 2. GRAVIMETRIC MEASUREMENTS

The measurement of  $g$  at the location of a FSM is only possible prior to its installation. Either absolute gravimeters (AG) are used on the location itself or relative gravimeters



Figure 1: FG5X-220 at PTB, Braunschweig.

are used to transfer a  $g$ -value from an absolute gravimeter point in close proximity. The force laboratory at PTB already holds an established relative gravimetric network [1], which was extended for this project. The network for this work shares three common points with the existing network. The observed gravity difference between the epochs of 2002 and 2015 is below  $20 \text{ nm/s}^2$ . In addition, two separate absolute gravimetric points are located in the same building: one point is part of the German national gravimetric base network of 1994, and a second point was established by the Institute of Geodesy (Institut für Erdmessung, IfE) in 2008. The latter point has been revisited annually with the FG5X-220 AG (see figure 1) described in [2]. The overall variation of  $g$  on this position is  $70 \text{ nm/s}^2$ ; from 2015 to 2016 the change is just  $10 \text{ nm/s}^2$ . The FG5X-220 has participated in international comparisons of absolute gravimeters every two years including the latest CCM-G.K2 [3, 4] and EURAMET.M.G-K2 [5] key comparisons in 2013 and 2015. The AG measurements provide the level of the gravimetric datum for the two relative gravimetric campaigns in May of



Figure 2: Lower part of the 200 kN FSM with gravimeter Scintrex CG3M-4492.

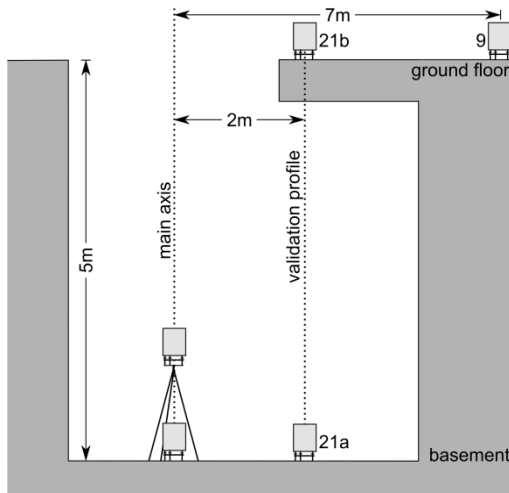


Figure 3: Gravimetric network in close proximity to the FSM. The main axis represents the center axis of the FSM deadweight stack.

2015 and July of 2016.

Prior to the installation of the new 200 kN FSM, described in another paper of this conference [6], the existing network was extended to include one point at the future position of the FSM as well as new points close to the FSM for the verification of its gravitational effect. The measurements were repeated in 2016 without the points now occupied by the FSM. Each relative gravimetric campaign was carried out with two gravimeters. In 2015, the gravimeters Scintrex CG3M-4492 and the ZLS Burris B-64, both of IfE, were used [7, 8] and in 2016, the CG3M-4492 was deployed together with CG3-3210 of Leibniz Institute for Applied Geophysics (LIAG). Figure 2 shows the CG3M-4492 on a tripod at the basement level of the FSM. A second position is 5 m vertically above this position on the ground floor level of the force laboratory. These points serve as a validation profile, which allows to examine the modelled

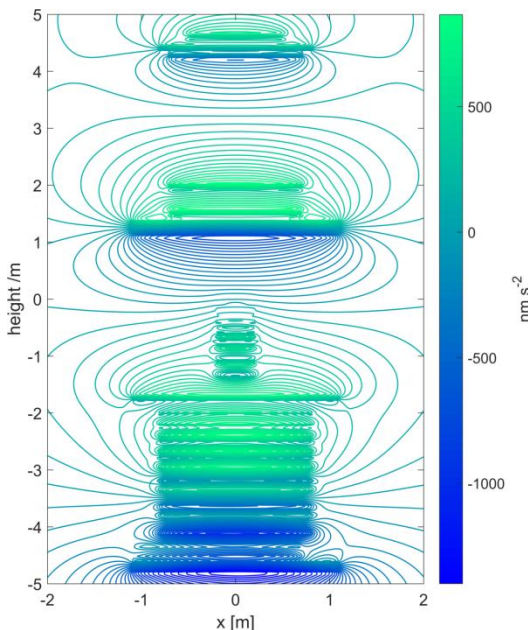


Figure 4: Gravitational effect of the FSM masses for a space containing the FSM (with a  $50 \text{ nm/s}^2$  contour line interval).

gravity changes by comparing it with the measurement results obtained before and after the installation of the FSM. A third point, still with a significant effect of the FSM, is about 7 m beside the FSM main vertical axis on the ground floor level. This network is shown in figure 3. Additionally, the vertical gravity gradient was measured at the FSM location. The points of the gravimetric network were connected by more than 110 measurements in each campaign and individual points were connected by about 10 measurements with each gravimeter to the network. The resulting standard deviations for the adjusted gravity differences were below  $20 \text{ nm s}^{-2}$  in all cases.

The AG points are more than 30 m away and are not affected by the FSM masses as measurable changes. Absolute  $g$  was measured over several nights with an uncertainty of  $25 \text{ nm/s}^2$ .

### 3. GRAVITY MODEL OF THE FSM

A simplified gravity model of the 200 kN FSM was generated from CAD construction plans. Tetrahedrons were used to calculate the Newtonian attraction as well as the vertical gradients [9]. Tetrahedrons were chosen because arbitrary shapes can be approximated easily and Delauny triangulation can be used to build the geometry for the model. However, the method described in [9] can be used for any geometric shape.

The masses of the 16 individual deadweights were determined at PTB with an expanded relative uncertainty of  $3 \times 10^{-6}$  [6]. The mass distribution of the support structure of the FSM was taken from the construction plans. An uncertainty of up to 2 percent of the weight can be assumed for the support structure. The shape of the support structure was simplified by omitting small recesses and by assuming a uniform density distribution. This resulted in closed bodies matching the outer dimensions and the weight according to the construction plans. With this model the gravitational effect can be determined for arbitrary positions.

### 4. RESULTS

The primary interest is the determination of the gravity effect of the FSM along the main axis of the mass stack. Secondly, the attraction at a distance of 2 m beside the main axis has been calculated. This is the closest position on which a relative gravimeter can be deployed (see figure 2). Overall, the not-modelled (residual contributions) of the FSM masses on the force measurement should be below the maximum contribution of the Earth tides.

Figure 4 shows the gravitational effect of the FSM model with a vertical plane including the machine's main axis. The height of 0 m is the ground floor of the FSM hall at PTB. The height of  $-5 \text{ m}$  is the basement level on which the machine stands. The first deadweight is at a height of approximately  $-4 \text{ m}$  and the topmost at 0 m. The regular structures in this area coincide with the positions of the individual deadweights. The center of the plot ( $x=0 \text{ m}$ ) is the main axis and the right border ( $x=2 \text{ m}$ ) is the reference profile, measured with relative gravimeters. The gravitational effects of the FSM's masses on the central axis

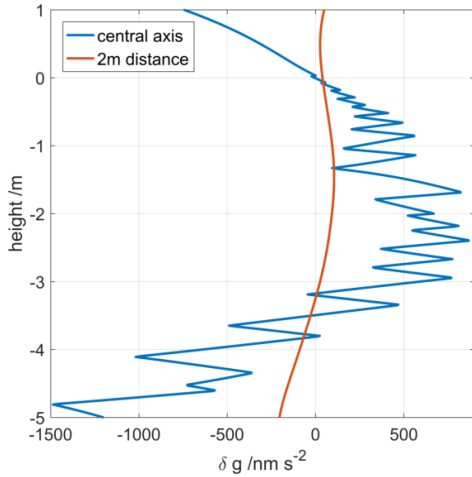


Figure 5: Effect on the main axis (blue) and 2 m beside the main axis (red) in the height range of the deadweights calculated in a 1 cm interval.

range from  $-1500 \text{ nm/s}^2$  to  $+1000 \text{ nm/s}^2$ . This is a relative effect of up to  $1 \times 10^{-7}g$  in the force measurement. In the following text we will focus on the lower part of the FSM, which contains the mass stack. The maximum amplitudes as derived by gravity modelling are given to indicate whether the respective quantity can be neglected. The calculations shown here were performed for the resting positions of the deadweights. The change of gravity at the center of mass of the upper (lower) weights is in the order of  $\pm 30 \text{ nm/s}^2$  ( $\pm 80 \text{ nm/s}^2$ ) after the weight has been shifted on the load frame, which changes its height slightly in relation to the remaining masses. Additionally, the gravity gradient has to be taken into account for the height change when the deadweights are lifted for a few cm by the load frame. Inside the deadweights between  $-4 \dots -2 \text{ m}$  the gradient is  $+10 \dots +20 \text{ nm s}^{-2}/\text{cm}$ . For the remaining weights between  $-1.5 \dots 0 \text{ m}$  the gradient varies between  $-20 \dots +20 \text{ nm s}^{-2}/\text{cm}$ . The combined effect for the individual  $g_i$  is below  $100 \text{ nm/s}^2$ . The computation of all individual combinations of deadweight positions on the load frame and in the resting position is unnecessary at this point.

Figure 5 shows the effect along the FSM main axis (blue line), where the change of  $g$  is needed for the force

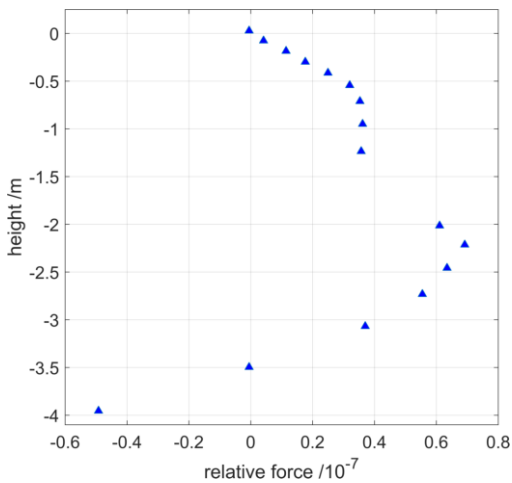


Figure 6: Impact on a force measurement at the center of mass of each deadweight.

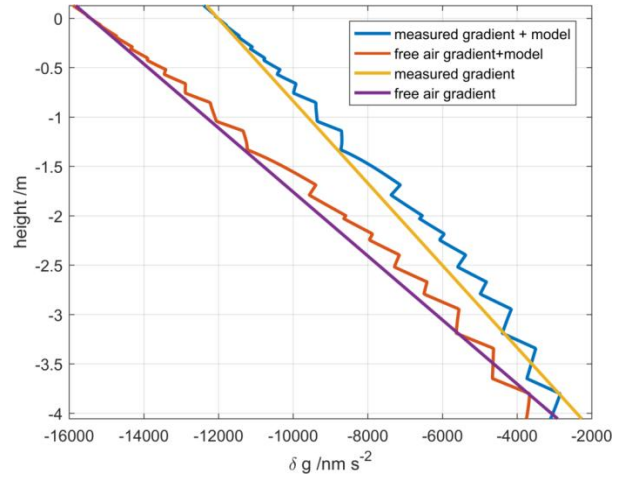


Figure 7: Height reduction applied to  $g$  (valid at basement level) along the main axis using the measured as well as the free air gradient and the modelled effect of the FSM.

measurement, and in a lateral distance of 2 m (red line). The zigzag structure on the main axis originates from the distribution of the individual masses of the FSM. In a distance of 2 m, the change of gravity is smoother and the amplitude of the signal is about  $200 \text{ nm/s}^2$  on the basement level and  $40 \text{ nm/s}^2$  on the ground floor. These magnitudes are detectable with modern relative gravimeters. The effect of the uncertainty of the weight of the FSM frame was determined by a simulation. In this simulation, the weights of the elements of the frame were changed randomly by up to 2 percent assuming a normal distribution. On the main axis, the effect on gravity is up to  $\pm 10 \text{ nm/s}^2$ ; 2 m beside the main axis the effect is reduced to  $\pm 1 \text{ nm/s}^2$ . The expanded uncertainty of the individual  $g_i$  is on average  $50 \text{ nm/s}^2$  ( $101 \text{ nm/s}^2$ ) for the upper (lower) mass stack. This considers the mass of the FSM frame, the relative positions of the individual deadweight (as opposed to the resting position) and the effect of the gradient. In a force measurement of the maximum force of the FSM the combined expanded uncertainty of all  $g_i$  due to the aforementioned three effects totals up to  $310 \text{ nm/s}^2$ .

Figure 6 shows the relative effect on a force measurement at the center of mass of each deadweight. The weights by themselves contribute with  $-0.5$  to  $+0.7 \times 10^{-7}$  relatively to the acting forces.

From the absolute gravity points, the  $g$ -value has been transferred to the floor point in the basement by relative gravimetry. Figure 7 shows reductions, which have to be applied to the floor  $g$ -value, to obtain  $g_i$  above the floor point along the central axis of the FSM. Considering only the free air gradient of  $-3086 \text{ nm s}^{-2}/\text{m}$  results in systematically too low  $g$  values in the heights of the deadweights. The measured gradient of  $-2320 \text{ nm s}^{-2}/\text{m}$  is only valid up to about 2 m above the basement level, where the gradient was measured. Above this height, the gradient would increase but not reach the free air gradient due to the complex environment (see also figure 3). The gradient measured on the validation profile is  $-2357 \text{ nm s}^{-2}/\text{m}$  over the full 5 m between basement and ground floor. The non-

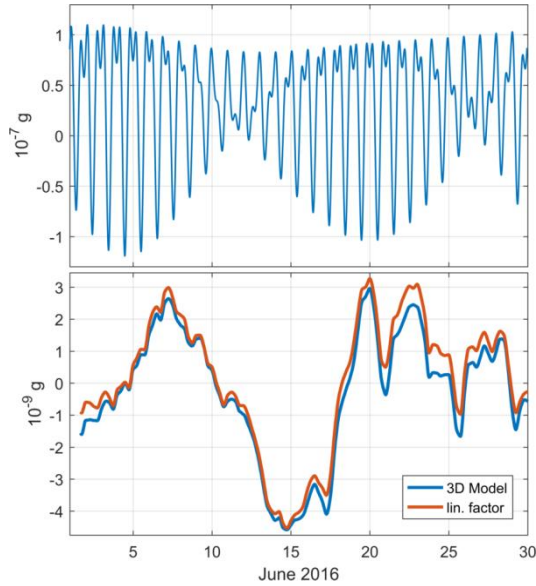


Figure 8: The relative effect on a force measurement at PTB due to Earth tides (*top*) and atmospheric mass variations (*bottom*) for one month.

linear components are not accounted for by the measurements.

If only a single gravity value is considered for all 16 deadweights, the effect of the FSM masses and the gravity gradients on the force measurements becomes very large. If only the  $g$ -value, which was transferred to the basement, is used, the  $g_i$  of the topmost deadweight would be off by  $-12000 \text{ nm/s}^2$  (compare figure 7). This is more than  $1 \times 10^{-6} g$  and the same order of magnitude as the uncertainty due to the determination of the weight. If  $g$  is chosen at the height of the center of mass of the whole mass stack, at about  $-3.17 \text{ m}$ , the neglected gravitational effect would range from  $-7400 \text{ nm/s}^2$  for the topmost deadweight to  $1900 \text{ nm/s}^2$  for the lowermost deadweight. At the mean height of the mass stack, approximately  $-1.52 \text{ m}$ , this range shifts to  $-3500 \dots 5700 \text{ nm/s}^2$ . At a height of  $-2 \text{ m}$  the effect would be below  $5 \times 10^{-7} g$  for all deadweights. Thus, the change of gravity with height cannot be neglected for a FSM of this extend, if the targeted uncertainty of  $g$  is to be limited by the Earth tides and not the gravity effect of the FSM.

Gravimetric point measurements before and after the FSM installation are used for verification of the forward modelling. Two of these points are  $2 \text{ m}$  beside the main axis on the basement level and the ground floor directly above one another. The calculated effect of the FSM for the gravity difference between these two points is  $-245 \text{ nm/s}^2$ . The

Table 1: Comparison of gravimetric measurements before and after the FSM installation and its modelling. See figure 3 for the location of the points. The differences are between epoch 2015 and 2016.  $Ex$  is one of the absolute gravimeter positions.

Difference	Model [ $\text{nm/s}^2$ ]	Measurement [ $\text{nm/s}^2$ ]
<b>21a – 21b</b>	-245	-237
<b>21b – 9</b>	26	36
<b>Ex – 21a</b>	205	194
<b>Ex – 9</b>	-14	-7

Table 2: Final gravity values and standard deviations (on the respective floor height) after the installation of the FSM from the 2016 measurement campaign.

Station	$g_{loc}$ [ $\text{nm/s}^2$ ]
<b>21a</b>	$9812530776 \pm 29$
<b>21b</b>	$9812518946 \pm 28$
<b>9</b>	$9812519329 \pm 26$
<b>200 kN FSM</b>	$9812529794 \pm 30$ (including the FSM mass modelling)

gravity effect between the two points on the ground floor has been calculated as a change of  $26 \text{ nm/s}^2$ . These computed values agree within  $10 \text{ nm/s}^2$  with the observed changes in the gravity differences between the measurement epochs in 2015 and 2016 (see table 1). These results correspond to the limit of accuracy provided by the relative gravimeters. The final gravity values after the FSM installation are presented in table 2. The given standard deviation is the result of the least squares network adjustment. The  $g_{loc}$  of the FSM and its standard deviation are derived from the 2015 AG measurement (with a standard deviation of  $25 \text{ nm/s}^2$ ), the connecting relative gravimetric measurement (with an average standard deviation of  $11 \text{ nm/s}^2$ ), the difference in the 2015/2016 AG measurements and the modelled FSM gravity effect.

It should be noted, that the determination of  $g_i$  is not the limiting factor of force measurements, therefore, a more comprehensive measurement campaign was not necessary. In future realizations of FSMs, especially in cases with mass stacks spanning several meters, gravimetric measurements at several points along the main axis of the machine can further improve the gravity value  $g_i$  determined inside the FSM.

The effect of the temporal variation of the gravity field caused by the Earth tides and atmospheric mass changes is shown in figure 8. The Earth tides have the largest relative effect of all phenomena discussed here for the 200 kN FSM. Within about six hours the full amplitude of up  $2.3 \times 10^{-7} g$  (peak to peak at PTB) of the Earth tides is passed. In fact, if not considered, the Earth tides contribute to the accuracy of the force measurement significantly with respect to the knowledge of  $g$ . To reduce this effect down to a few percent, depending on the location and its proximity to the coast, a procedure is provided by, e. g., [10]. This method could be implemented in the software of the FSM. A more complete reduction requires the knowledge about amplitude and phases of the main partial tides for the FSM site, which is provided by, e. g., [11] or by gravimetric observations.

The effect of atmospheric mass changes is shown in the bottom plot of figure 8. The overall relative effect only reaches  $4 \times 10^{-9} g$ . When calculating this effect under consideration of a global 3D model of the atmosphere instead of the linear factor of  $3 \text{ nm/s}^2/\text{hPa}$  [12], the improvement is about  $1 \times 10^{-9}$ . The effect of local hydrology is not shown due to the lack of data. But the relative effect is at the order of  $1 \times 10^{-8} g$  for a groundwater level change of  $1 \text{ m}$  assuming a Bouguer plate and a porosity of 30 % of the soil.

## 5. SUMMARY

We determined the gravitational effect of the new 200 kN FSM at PTB modelled with tetrahedrons. The individual  $g_i$  for the center of mass of each deadweight is derived from a combination of this model and gravimetric measurements. Currently, the model only considers the static case. The effect on  $g_i$  by lifting different combinations of masses with the load frame is below  $1 \times 10^{-8}$  of the generated force. The model was compared to gravimetric measurements taken prior and after the installation of the FSM. Model and measurements agree within  $10 \text{ nm/s}^2$ , which is also the limit of modern spring gravimeters. This comparison with measured results is only possible outside of the machine, therefore a vertical profile 2 m beside the main axis of the FSM was chosen. A second, horizontal profile shows the same agreement between model and observations. A further improvement of the model, e.g., a more complex geometry, cannot be verified with state-of-the-art spring gravimeters. Furthermore, a better model and more extensive measurements are not necessary, because the uncertainties in  $g_i$  are not the determining limitation in force measurements.

For practical applications, the gravity values  $g_i$  along the central axis of the FSM should be calculated by correcting the influence of the FSM masses on the floor point with  $1136 \text{ nm/s}^2$  (see figure 5 and table 2). Additionally, the measured gradient  $-2320 \text{ nm s}^{-2}/\text{m}$  should be used (see figure 7) to transfer the  $g_{loc}$  from the floor of the basement to the center of mass of the individual deadweight.

The effect of temporal changes to  $g$ , dominated by the Earth tides, was estimated. Once these effects become relevant, the influence of the Earth tides can be reduced to a few  $10^{-9}$  by a rather simple method, implemented in the FSM software.

With the described method and the not considered temporal variations a relative uncertainty in the order of  $1.2 \times 10^{-7} g$  can be ensured for the position of the center of masses within the deadweights. With a tidal correction the uncertainty can be reduced to  $1 \times 10^{-8}$  in  $g$ .

**Acknowledgement:** The authors thank the Leibniz Institute for Applied Geophysics (LIAG) for providing the CG3-3210 gravimeter for the second measurement campaign.

## 6. REFERENCES

- [1] A. Lindau, R. Kumme, A. Heiker, "Investigation in the local gravity field of a force laboratory of PTB", VDI Berichte, vol. 1685, pp. 589-598, 2002.
- [2] T. M. Niebauer, R. Billson, A. Schiel, D. van Westrum, F. Klopping, "The self-attraction correction for the FG5X absolute gravity meter", Metrologia, vol. 50, no. 1, pp. 1-8, 2013.
- [3] M. Schilling, L. Timmen, "Traceability of the Hannover FG5X-220 to the SI units", International Association of Geodesy Symposia, doi: 10.1007/1345\_2016\_226, 2016.
- [4] O. Francis, H. Baumann, C. Ulrich, S. Castelein, M. Van Camp et al., "CCM.G-K2 Key Comparison", Metrologia, vol. 52, pp. 07005, 2015.
- [5] V. Pálinkáš, O. Francis, M. Val'ko, J. Kostecký, M. Van Camp et al., "Regional comparison of absolute gravimeters, EURAMET.M.G-K2 key comparison", Metrologia, vol. 54, pp. 07012, 2017.
- [6] R. Kumme, H. Kahmann, F. Tegtmeier, N. Tetzlaff, D. Röske, "PTB's new 200 kN deadweight force standard machine", to be published in Proc. of IMEKO 23rd TC3, 13th TC5 and 4th TC22 International Conference, Helsinki, 2017.
- [7] L. Timmen, O. Gitlein, "The capacity of the Scintrex Autograv CG-3M no. 4492 gravimeter for "absolute -scale" surveys", Revista Brasileira de Cartografia, vol. 56, no. 2, pp. 89-95, 2004.
- [8] M. Schilling, O. Gitlein, "Accuracy estimation of the IfE gravimeters Micro-g LaCoste gPhone-98 and ZLS Burris Gravity Meter B-64", International Association of Geodesy Symposia, vol. 143, pp. 249-256, 2015.
- [9] V. Pohanka, "Optimum expression for computation of the gravity field of a homogeneous polyhedral body", Geophysical Prospecting, vol. 36, no. 7, pp. 733-751, 1988.
- [10] I. M. Longman, "Formulas for computing the tidal accelerations due to the Moon and the Sun", Journal of Geophysical Research, vol. 64, no. 12, pp. 2351-2355, 1959.
- [11] L. Timmen and H.-G. Wenzel, "Worldwide synthetic gravity tide parameters", International Association of Geodesy Symposia, vol. 113, pp. 92-101, 1995.
- [12] IGC, "International Absolute Gravity Basestation Network (IAGBN), Absolute Gravity Observations, Data Processing, Standards & Station Documentation (Int. Grav. Com.-WGII: World Gravity Standards)," Bureau Gravimetricque International, Bulletin d'Information, vol. 63, pp. 51-57, 1988.